The Effect of Surface Chemistry of Graphene on Cellular Structures and Electrical Properties of Polycarbonate Nanocomposite Foams

ARTICLE *in* INDUSTRIAL & ENGINEERING CHEMISTRY RESEARCH · MARCH 2014

Impact Factor: 2.59 · DOI: 10.1021/ie4039899

6 AUTHORS, INCLUDING:

Hao-Bin Zhang
Beijing University of Chemical Technology
26 PUBLICATIONS **970** CITATIONS
SEE PROFILE

Xiaofeng Li
Beijing University of Chemical Technology
32 PUBLICATIONS **414** CITATIONS
SEE PROFILE

I&EC research
Industrial & Engineering Chemistry Research

Article

pubs.acs.org/IECR

The Effect of Surface Chemistry of Graphene on Cellular Structures and Electrical Properties of Polycarbonate Nanocomposite Foams

Hui-Ling Ma,[†,‡] Hao-Bin Zhang,*[,†] Xiaofeng Li,[†] Xin Zhi,[†] Yong-Fei Liao,[†] and Zhong-Zhen Yu*[,†]

[†]State Key Laboratory of Organic−Inorganic Composites, Beijing University of Chemical Technology, Beijing 100029, China
[‡]Beijing Research Center for Radiation Application, Beijing Academy of Science and Technology, Beijing 100015, China

Supporting Information

ABSTRACT: Electrically conductive polycarbonate (PC) nanocomposites are prepared by blending PC with thermally exfoliated graphene and p-phenylenediamine (PPD)-functionalized and reduced graphene oxide (GO-PPD). The filler dispersion in the PC matrix is evaluated with scanning electron microscopy, transmission electron microscopy, and rheological measurements. Compared to thermally exfoliated graphene, GO-PPD exhibits a better compatibility with the PC matrix and thus a more homogeneous dispersion due to the presence of PPD in GO-PPD. After being freely foamed with supercritical carbon dioxide as the foaming agent, the PC/GO-PPD nanocomposite foams show improved cell structures with higher cell density, smaller cell size, and more regular shapes; these should be attributed to the uniform dispersion of GO-PPD sheets in the matrix, which act as nucleation sites for foaming. Interestingly, the conducting network formed by GO-PPD sheets survives even after mold-limited foaming of PC/GO-PPD nanocomposites, and therefore the nanocomposite foams exhibit similar or even higher electrical conductivity in comparison to their solid counterparts.

1. INTRODUCTION

Polymer nanocomposite foams have recently attracted increasing interest in both the scientific and industrial communities.[1−6] The incorporation of functional nanofillers not only reinforces polymer foams but also functionalizes the foams at a low loading of nanofillers.[6−8] Compared to conventional fillers, nanofillers have their advantages in fabricating microcellular foams with improved specific strength,[8] increased toughness,[1] and high thermal stability;[9−12] this is because nanofillers could provide numerous heterogeneous nucleation sites due to their large specific surface area and high aspect ratios, optimize the cellular structures, and reinforce the cell walls.[8,13]

Layered silicates have been employed to enhance the tensile strength, fracture toughness and thermal properties of polymer foams due to their versatile and tunable chemical composition.[6,14,15] The effects of their dispersion, surface chemistry, and interfacial interactions with polymer matrices on cell morphology and properties of polymer foams have been extensively explored.[13,14,16−18] To fabricate polymer foams for antistatic and electromagnetic interference (EMI) shielding applications, carbon nanofillers including carbon fibers (CNFs) and carbon nanotubes (CNTs) are preferred in the pioneering work of Yang and co-workers.[1−4,19,20] By controlling the aspect ratio and surface chemistry of CNTs and their dispersion in polymer matrices, the nucleation mechanism, cell structures, and properties of the polymer foams could be tailored.[7,21−23]

As a layered and functional nanofiller, graphene is still rarely utilized in polymer foams, although its solid nanocomposites have been extensively studied.[5,24−26] We developed an approach to prepare functional poly(methyl methacrylate) (PMMA)/graphene nanocomposite foams by blending PMMA with graphene followed by foaming with subcritical carbon dioxide as an environmentally benign foaming agent.[1] The resultant nanocomposite foams exhibited not only high electrical and EMI shielding performances but also greatly enhanced ductility and tensile toughness.[1] Recently, polystyrene/graphene and poly(ether imide)/graphene nanocomposite foams were prepared using different foaming methods, and impressive EMI shielding properties were obtained.[27−29] Highly conductive polymer foams using preformed three-dimensional interconnected graphene network structures were also prepared.[30−32] Besides, graphene oxide (GO) was used to modify polystyrene foams, but only slight cellular structure changes were observed.[33] Overall, GO and its derivatives are promising nanofillers in the preparation of polymer nanocomposites due to the simple preparation procedure and the mass production potential. The purpose of the present work is to study the influence of surface chemistry of graphene and GO on cellular morphology and electrical properties of their polycarbonate (PC) nanocomposite foams. Both p-phenylenediamine (PPD)-functionalized and reduced GO (GO-PPD) and thermally exfoliated graphene were used as conductive nanofillers. The resultant PC nanocomposites were freely or mold-limited foamed by a batch foaming process with supercritical carbon dioxide as the foaming agent. The effects of surface chemistry and content of the nanofillers on their dispersion in the PC matrix, cell morphology, and electrical properties of the nanocomposite foams were investigated.

2. EXPERIMENTAL SECTION

Materials. Natural graphite flakes (∼13 μm) were purchased from Huadong Graphite Factory (China). Makrolon

Received: November 25, 2013
Revised: February 28, 2014
Accepted: March 6, 2014
Published: March 6, 2014

   dx.doi.org/10.1021/ie4039899 | Ind. Eng. Chem. Res. 2014, 53, 4697−4703

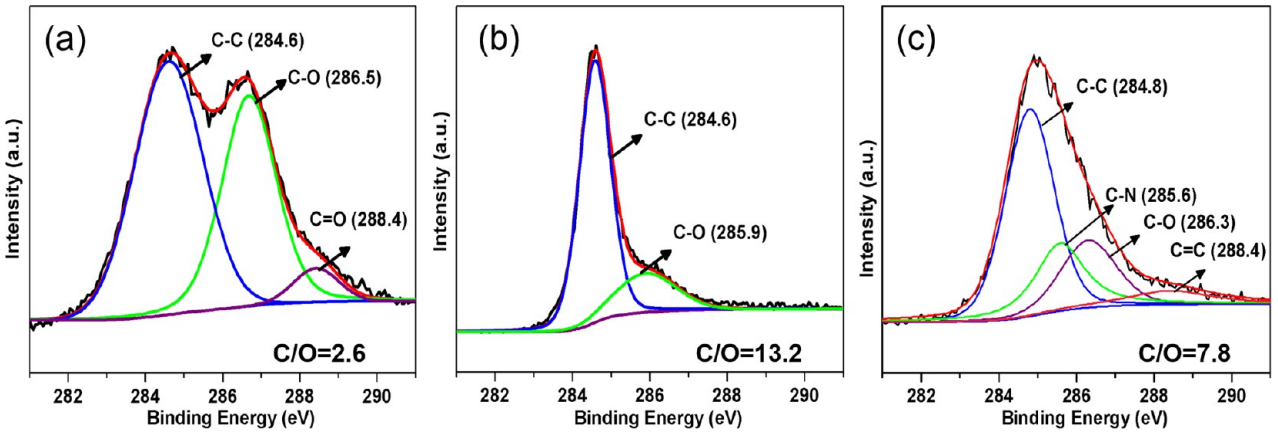

Figure 1. C 1s XPS spectra of (a) GO, (b) graphene, and (c) GO-PPD.

PC was provided by Bayer Company (Germany). PPD was purchased from Tianjin Guangfu Fine Chemical Research Institute (China). Sodium nitrate was bought from Xilong Chemical Industry (China). Potassium permanganate (99.5%), methylene dichloride, and all the other reagents and solvents were purchased from Beijing Chemical Factory (China) and used as received.

Preparation of PC Nanocomposites. To investigate the effect of surface chemistry of graphene sheets on the microstructure and properties of PC nanocomposites, two types of graphene sheets are used. Thermally exfoliated graphene was obtained by thermal exfoliation and reduction of GO at 1050 °C,[1,26,34] while GO-PPD was prepared by simultaneous functionalization and reduction of GO with PPD at 95 °C for 3 h.[35] PC nanocomposites with graphene or GO-PPD were fabricated by solution compounding. For example, PC and graphene were separately dispersed in methylene dichloride by ultrasonication, and the graphene suspension was then mixed with PC solution followed by mechanical stirring with an IKA T18 homogenizer (Germany) for 2 h. The homogeneous mixture was poured into a petri dish and dried in an air-circulating oven at 80 °C for 12 h and a vacuum oven at 120 °C for another 12 h. Finally, PC nanocomposites were compression-molded into plates at 265 °C for 20 min using a Beijing Kangsente KT-0906 vacuum hot-press (China).

Preparation of PC Nanocomposite Foams. PC nanocomposite foams were prepared by a batch foaming process with supercritical carbon dioxide as the foaming agent, where bulk samples experienced saturation and foaming processes to get foamed with or without limitation. For free foaming, PC/graphene and PC/GO-PPD nanocomposites were saturated at 100 °C and 10 MPa for 6 h without any mold limitation. Subsequently, the high pressure was rapidly released and the samples were quickly immersed in a preheated hot oil at 170 °C for 10 s to induce the bubble nucleation and growth. To get flat and regular samples, molds were used to constrain the buckling deformation during the limited foaming process (mold-limited foaming). However, the usage of molds would make it difficult for solid PC and its nanocomposites to absorb adequate CO_2 and nucleate bubbles rapidly, the samples were thus saturated at higher pressure (13.8 MPa) and 100 °C for 6 h followed by foaming at 170 °C for a longer foaming time of 60 s.

Characterizations. The surface chemistry of GO, thermally exfoliated graphene, and GO-PPD was analyzed with a ThermoVG RSCAKAB 250X X-ray photoelectron spectroscope (XPS). A Hitachi S-4700 scanning electron microscope (SEM) and Hitachi H-800 transmission electron microscope (TEM) were employed to observe the microstructures of PC nanocomposites and foams. Rheological behaviors of PC and its nanocomposites were measured with a TA Instruments ARES-G2 strain-controlled rheometer. The volume conductivities of the samples with higher conductivities than 1×10^{-4} S/m were measured with a 4-Probes-Tech RTS-8 four-probe resistivity meter (China), whereas the samples with lower conductivity than 1×10^{-4} S/m were measured by a ZC-90G resistivity meter from Shanghai Taiou Electronics (China). Image-pro plus software was used to determine the cell sizes, and the average sizes were calculated based on more than 200 cells in the selected SEM images. The cell number per unit volume (N) was calculated based on eq 1:[36,37]

$$N = \left(\frac{nM^2}{A}\right)^{3/2} \tag{1}$$

where n is the number of cells in the selected SEM image of PC foams, M is the magnification, and A is the area of the SEM image.

3. RESULTS AND DISCUSSION

3.1. Functionalization of Graphene and Its PC Nanocomposites. The surface chemistry of GO, thermally exfoliated graphene and GO-PPD was analyzed with XPS (Figure 1). The fitted curves of GO indicate the presence of an unoxidized graphite carbon skeleton (284.6 eV), C−O in the hydroxyl group and epoxide group (286.5 eV) and C═O in the carboxyl group (288.4 eV) (Figure 1a). However, the C 1s XPS spectrum of thermally exfoliated graphene is greatly narrowed, and only a weak peak assigned to C−O in the hydroxyl group and epoxide group is observed (Figure 1b), which implies that most of the oxygen functionalities are removed during the high temperature shock, evidenced by its much higher C/O ratio of 13.2 relative to 2.6 for GO. Similarly, only one characteristic peak is observed for GO-PPD, and most of its fitted peaks corresponding to oxygen functionalities are greatly weakened in comparison to that of GO (Figure 1c). Combined with the UV−vis absorption and Fourier-transform infrared spectroscopy results described elsewhere,[35] the reduction of GO during the refluxing in the presence of PPD is confirmed, although the C/O ratio (7.8) of GO-PPD is lower than that of thermally exfoliated graphene. The higher amount of the residual oxygen-containing groups in GO-PPD would facilitate its dispersion in polar polymer matrix. Additionally, the appearance of a new

dx.doi.org/10.1021/ie4039899 | Ind. Eng. Chem. Res. 2014, 53, 4697−4703

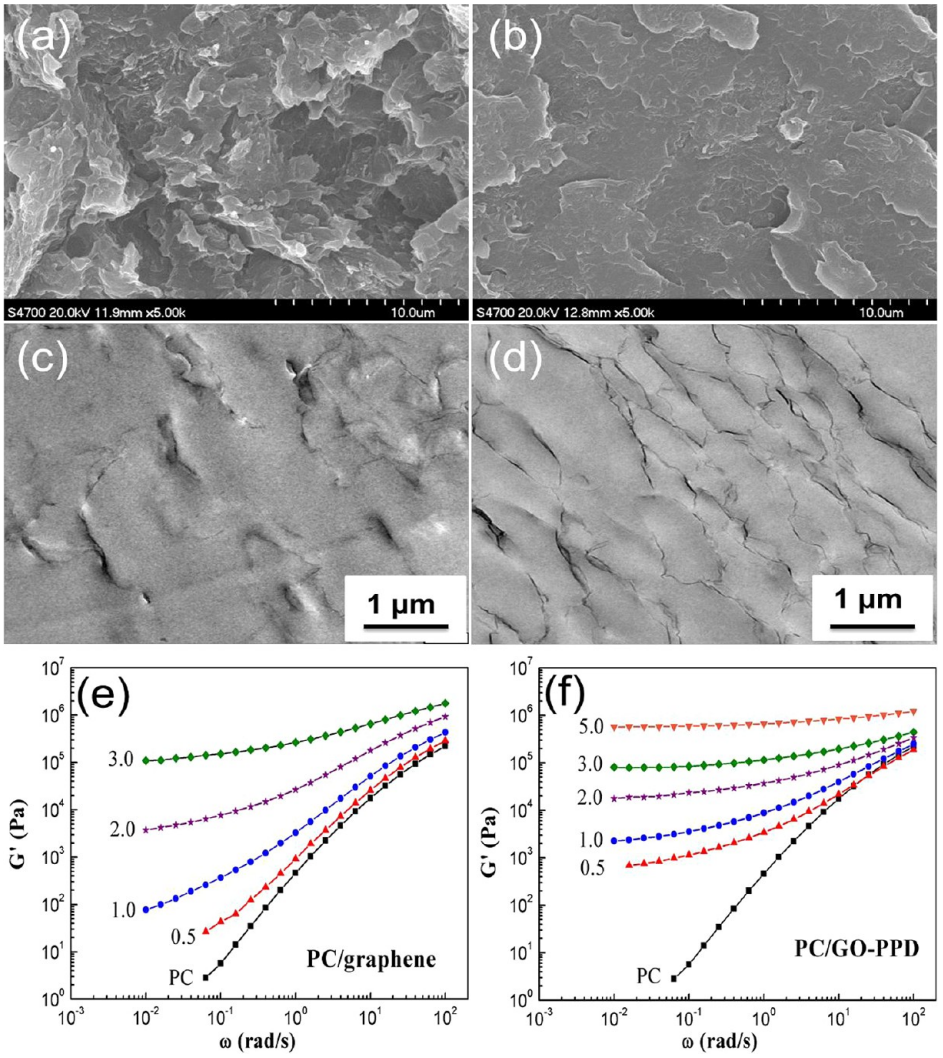

Figure 2. SEM images of fracture surfaces of (a) PC/2 wt % graphene and (b) PC/2 wt % GO-PPD nanocomposites. TEM images of (c) PC/2 wt % graphene and (d) PC/2 wt % GO-PPD nanocomposites. Plots of storage modulus versus frequency for (e) PC/graphene and (f) PC/GO-PPD nanocomposites at 250 °C.

peak centered at 285.6 eV, assigned to C−N, confirms the functionalization of GO with PPD by the chemical reaction between the amine groups of PPD and the epoxide groups of GO. The presence of PPD would prevent the aggregation of GO-PPD sheets and improve their dispersion in the PC matrix.[35]

To investigate the effect of chemical components of graphene and GO-PPD sheets on their dispersion in PC matrix, Figure 2 shows the SEM and TEM images of PC/graphene and PC/GO-PPD nanocomposites. The PC/graphene nanocomposite presents a rough microstructure with large pores, while the PC/GO-PPD nanocomposite displays a smooth fracture surface (Figures 2a and b), suggesting distinct dispersion of the nanofillers. More careful observation with TEM reveals slight aggregations of the thermally exfoliated graphene sheets in the PC/graphene nanocomposite, whereas GO-PPD sheets are well dispersed and an interconnecting network is formed in the PC/GO-PPD nanocomposite (Figures 2c and d). It is clear that the functionalization of GO with PPD results in a finer dispersion of GO-PPD in the PC matrix in comparison with the thermally reduced graphene.

To further evaluate the distribution of graphene in the matrix, the dynamic frequency-sweep measurements of the PC nanocomposites are performed at 250 °C because of the high sensitivity of rheological properties to the filler dispersion in polymer composites.[19,38,39] Figure 2e and f show the plots of storage modulus versus frequency for PC/graphene and PC/GO-PPD nanocomposites at 250 °C. At a low loading of 0.5 wt %, GO-PPD is more efficient in enhancing the storage modulus of PC than thermally exfoliated graphene. The storage modulus of PC/GO-PPD nanocomposites becomes essentially independent of frequency in the low-frequency range when the loading of GO-PPD is more than 0.5 wt %. This indicates the earlier transition from a liquid-like to a solid-like viscoelastic behavior and the formation of an interconnecting network in a PC matrix, which would restrict the long-range motion of polymer chains and contribute to the nonterminal behavior of PC nanocomposites. In contrast, the addition of 0.5 wt % thermally exfoliated graphene only results in a moderate increase in storage modulus for the PC/graphene nanocomposite and the plateau, implying that the formation of an interconnecting network appears at a high loading of 2.0 wt %. The earlier formed interconnecting network and the higher

dx.doi.org/10.1021/ie4039899 | Ind. Eng. Chem. Res. 2014, 53, 4697−4703

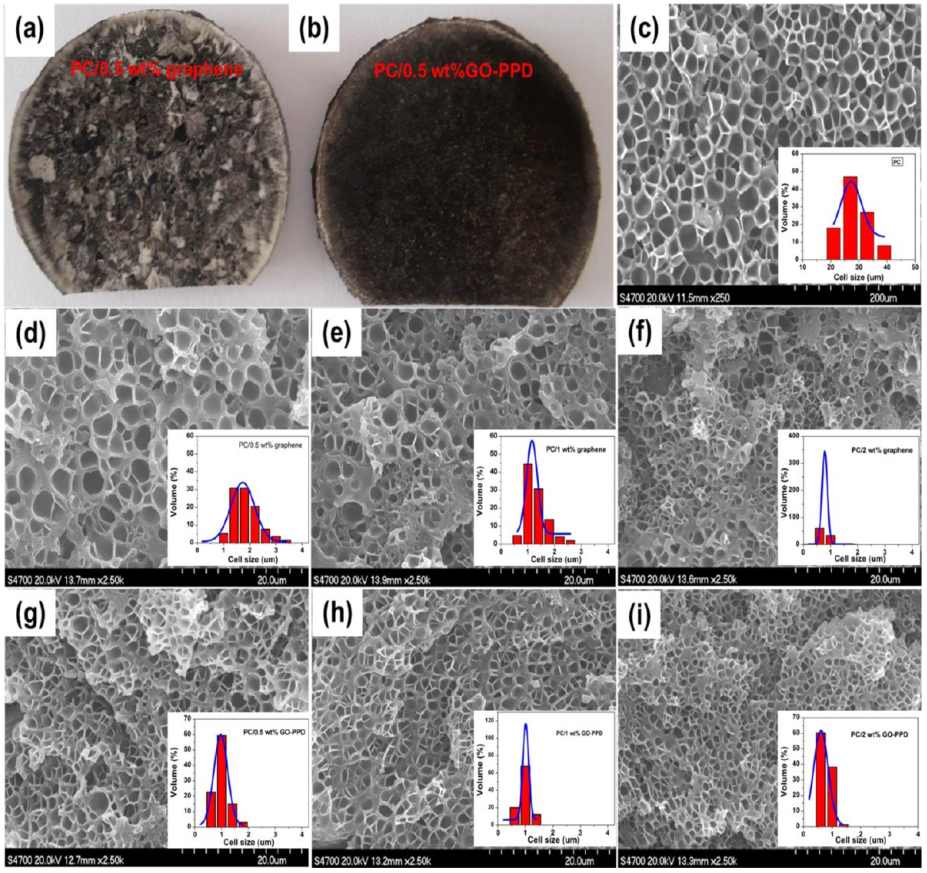

Figure 3. Digital images of (a) PC/0.5 wt % graphene and (b) PC/0.5 wt % GO-PPD nanocomposite foams. Cell morphologies of (c) neat PC foam, (d) PC/0.5 wt % graphene foam, (e) PC/1 wt % graphene foam, (f) PC/2 wt % graphene foam, (g) PC/0.5 wt % GO-PPD foam, (h) PC/1 wt % GO-PPD foam, and (i) PC/2 wt % GO-PPD foam. The insets in c–i are size distribution of the cells. Scale bars are 200 μm for c and 20 μm for d–i.

storage modulus for PC/GO-PPD nanocomposites should be attributed to the better dispersion of GO-PPD sheets in the PC matrix than that of the thermally exfoliated graphene.

3.2. The Influence of Graphene on Cell Structures of PC Nanocomposite Foams. As previously reported,[6−8,14,18,21−23,29] nanofillers, such as clay, CNFs, CNTs, and graphene, would alter the nucleation mode and cell microstructure during the foaming process. PC nanocomposite foams filled with graphene and GO-PPD exhibit different appearances as indicated by the photographs in Figure 3a and b. The better dispersed GO-PPD results in a more uniform surface in contrast to the uneven texture of PC/graphene nanocomposite foam. The microstructure and cell morphology of the PC foams prepared by free-foaming are observed with SEM (Figures 3c–f), and the calculated average cell sizes and cell densities are listed in Figure 4.

Neat PC foam has an average cell size of 28.2 μm and a cell density of 7.8×10^7 cells/cm^3 (Figures 3c and 4). However, the addition of 0.5 wt % graphene leads to a much smaller cell size of 1.8 μm and a much larger cell density of 5.2×10^{10} cell/cm^3, which is nearly 3 orders of magnitude higher than that of neat PC foam. With 1 wt % of graphene, the cell size decreases to 1.3 μm and cell density increases to 1.2×10^{11} cell/cm^3. When the content of graphene increases to 2 wt %, the cell size is further reduced to 0.77 μm, and the cell density is increased to 4.2×10^{11} cell/cm^3. Therefore, these results indicate the efficient heterogeneous nucleation effect of graphene and its significant impact on cell structure of PC foams. As previously

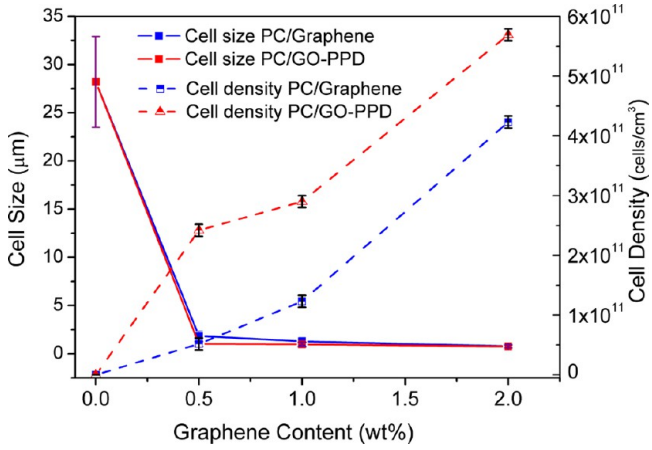

Figure 4. Comparison of cell size and cell density of PC nanocomposite foams filled with graphene and GO-PPD.

reported, the number and size of bubbles depend on the concentration of the foaming agent.[16,40] In the PC/graphene nanocomposites, the increase of graphene content leads to larger interfacial areas for carbon dioxide absorption and cell nucleation, and thereby the nucleation rate and cell density are subsequently increased. Simultaneously, the cell size is also decreased because there are more nucleated sites to consume the given amount of gas.

dx.doi.org/10.1021/ie4039899 | Ind. Eng. Chem. Res. 2014, 53, 4697−4703

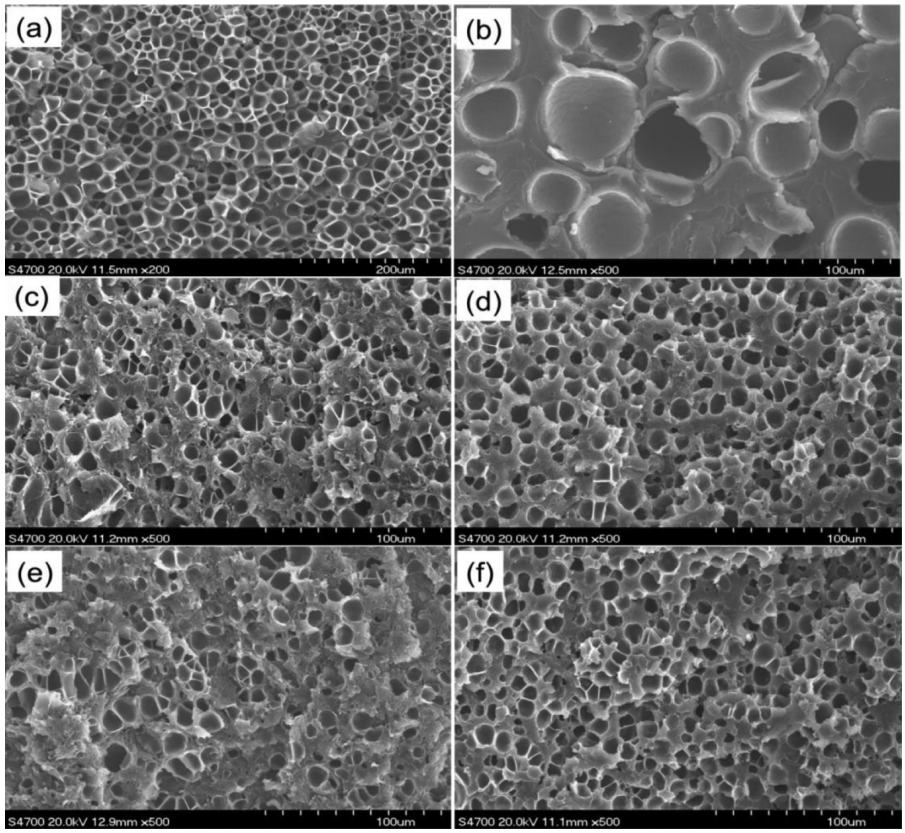

Figure 5. Cell structures of neat PC foams from (a) free and (b) limited foaming process, (c) PC/1 wt % graphene, (d) PC/1 wt % GO-PPD, (e) PC/2 wt % graphene, and (f) PC/2 wt % GO-PPD nanocomposite foams. Foam a was prepared at 13.8 MPa and 100 °C by free foaming and the other foams at 13.8 MPa and 100 °C by limited foaming with a mold. Scale bars are 200 μm for a and 100 μm for b–f.

Larger cell number and smaller cell size are observed in PC/GO-PPD nanocomposite foams in comparison to those of PC/graphene counterparts (Figures 3 and 4). The cell size of PC/0.5 wt % GO-PPD nanocomposite foam is only 1.0 μm, smaller than 1.8 μm for the PC/0.5 wt % graphene foam. The cell density (2.4×10^{11} cell/cm^3) of the former is 4 times higher than that of the latter. Moreover, the cells in the PC/0.5 wt % GO-PPD nanocomposite foam are more uniform with a narrower cell size distribution than those of its counterparts, as illustrated in the insets of Figures 3d–f. The smallest average cell size of 0.8 μm and the largest cell density of 5.7×10^{11} cell/cm^3 are achieved for the PC/2 wt % GO-PPD nanocomposite foam. It is clear that the well-dispersed GO-PPD serves as a more efficient heterogeneous nucleating agent in contrast to graphene during the foaming process, because the homogeneously distributed GO-PPD sheets generate larger amounts of PC/sheet interfaces and thus more available nucleation sites for foaming.[6,41]

3.3. The Influence of Mold-Limited Foaming on Cell Morphology of PC Nanocomposite Foams. Flat and regular shapes are required for the property measurements of polymer foams, and thus the buckling deformation of samples should be inhibited during the foaming. Figure 5a and b compare the cell structures of PC foams prepared by free-foaming and mold-limited foaming. The mold-limited foaming generates increased cell size (32.7 μm) and dramatically reduced cell density of 4.7×10^6 cell/cm^3 from 7.8×10^7 cells/cm^3 for free foaming. Similar changes are observed for the PC nanocomposite foams. The heterogeneous effect of graphene sheets during the foaming is also significant in the mold-limited foaming process, and thus the resulting nanocomposite foams exhibit much smaller cell size and higher cell density than neat PC foam.

Consistent with the results for the freely foamed materials, different cellular structures are also observed in the PC/GO-PPD and PC/graphene foams prepared by mold-limited foaming. The well dispersed GO-PPD induces a large number of heterogeneous nuclei and the simultaneous growth of the cells, and thus the PC/GO-PPD foam presents relatively uniform cell sizes with a narrow size distribution (Figure 5d and f). Nevertheless, the PC/graphene foam shows a typical bimodal cell morphology with some smaller (~1.3 μm) cells surrounded by bigger ones (~7 μm; Figure 5c and e). This bimodal morphology becomes more obvious when the graphene content is increased to 3.0 wt % (Figure S1). Additionally, the locations of cells are not well-distributed, and large-cell rich areas and small-cell rich areas are observed in the SEM image. The relatively poor dispersion of the thermally exfoliated graphene and its aggregates would be responsible for the graphene rich area and deficient area, where heterogeneous and homogeneous nucleation occur and the cells with various sizes are formed. Similar bimodal cell morphology has been previously reported for ethylene vinyl acetate and PMMA foams filled with CNTs, and it was also believed to be due to the simultaneous homogeneous and heterogeneous nucleation mechanisms.[1,7]

3.4. Electrical Properties of PC Nanocomposite Foams. Figure 6 compares the electrical conductivities of PC nanocomposites filled with graphene and GO-PPD before and after foaming. In spite of the relatively poor dispersion of

dx.doi.org/10.1021/ie4039899 | Ind. Eng. Chem. Res. 2014, 53, 4697–4703

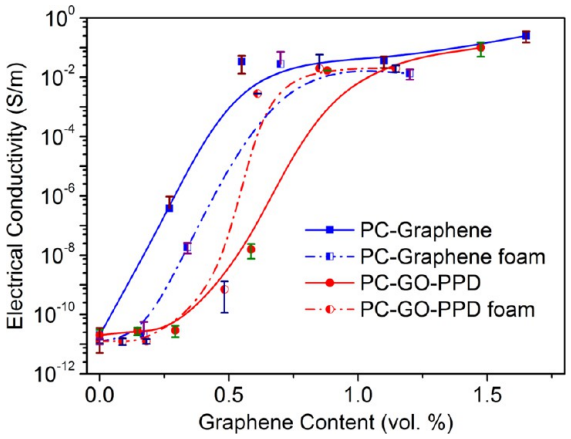

Figure 6. Plots of electrical conductivity versus nanofiller content for PC/graphene and PC/GO-PPD nanocomposites before and after foaming.

graphene, its PC nanocomposites exhibit higher electrical conductivities than PC/GO-PPD nanocomposites, especially at low loading of the nanofillers, which may be due to the much higher reduction extent of the thermally exfoliated graphene at 1050 °C than the chemically reduced GO-PPD. As previously reported, the electrical properties of foamed materials are considerably dependent on their bulk counterparts.[1−5] The electrical conductivity of a PC/graphene system decreases after foaming even if taking the volume of the generated bubbles into account. Whereas, the PC/GO-PPD foams exhibit similar electrical conductivities at low loadings and even higher conductivities at high loadings compared to their bulk counterparts. The different changes of the electrical properties upon foaming may result from the distinct filler dispersion and cell structures. The relatively poorly dispersed graphene only leads to a fragile conducting network, and the generated voids can easily interrupt the interconnection of the sheets and thus reduce the conductivity. However, the compact interconnecting network formed by chemically modified GO-PPD survives after foaming; as a result, the electrical conductivity of the nanocomposite foam is maintained or even improved due to the volume-exclusion effect of the bubbles.[1] Note that the optimized cell structures of the PC/GO-PPD foams would also contribute to the high electrical conductivity.

4. CONCLUSION

PC/graphene and PC/GO-PPD nanocomposite foams are prepared by a batch foaming process using supercritical carbon dioxide as the foaming agent. The SEM, TEM, and rheological results suggest that the improved compatibility of GO-PPD with a PC matrix results in a uniform distribution of GO-PPD. Both GO-PPD and graphene sheets act as effective heterogeneous additives benefiting the fabrication of microcellular nanocomposite foams with reduced cell sizes and improved cell densities. Compared to the unmodified graphene, the well-dispersed GO-PPD affords improved cell structures with further enhanced cell density and reduced cell size with a narrower cell size distribution during the free-foaming process. After mold-limited foaming, the PC/GO-PPD foams still exhibit evenly distributed cells with uniform cell sizes. However, a typical bimodal cell morphology is observed in the PC/graphene foams due to the simultaneous homogeneous and heterogeneous nucleation mechanisms. Furthermore, PC/GO-PPD foams show similar or even higher electrical conductivity compared to their bulk counterparts, while a slight decrease is observed for the PC/graphene nanocomposites after foaming. The better dispersion of GO-PPD sheets and improved cell structures of the PC/GO-PPD nanocomposite foams are responsible for the improved electrical properties.

■ ASSOCIATED CONTENT

Supporting Information

Bimodal cell morphology of PC/3 wt % graphene nanocomposite foam is provided. This material is available free of charge via the Internet at http://pubs.acs.org.

■ AUTHOR INFORMATION

Corresponding Authors

*Tel.: +86-10-6442 8582. Fax: +86-10-6442 8582. E-mail: zhanghaobin@mail.buct.edu.cn.

*Tel.: +86-10-6442 8582. Fax: +86-10-6442 8582. E-mail: yuzz@mail.buct.edu.cn.

Notes

The authors declare no competing financial interest.

■ ACKNOWLEDGMENTS

Financial support from the National Natural Science Foundation of China (51103007, 51125010, and 51373011) and the Specialized Research Fund for the Doctoral Program of Higher Education of China (20100010110006) is gratefully acknowledged.

■ REFERENCES

(1) Zhang, H. B.; Yan, Q.; Zheng, W. G.; He, Z.; Yu, Z. Z. Tough graphene-polymer microcellular foams for electromagnetic interference shielding. *ACS Appl. Mater. Interfaces* **2011**, *3*, 918.

(2) Yang, Y. L.; Gupta, M. C.; Dudley, K. L.; Lawrence, R. W. Conductive carbon nanoriber-polymer foam structures. *Adv. Mater.* **2005**, *17*, 1999.

(3) Yang, Y. L.; Gupta, M. C. Novel carbon nanotube-polystyrene foam composites for electromagnetic interference shielding. *Nano Lett.* **2005**, *5*, 2131.

(4) Xu, X. B.; Li, Z. M.; Shi, L.; Bian, X. C.; Xiang, Z. D. Ultralight conductive carbon-nanotube-polymer composite. *Small* **2007**, *3*, 408.

(5) Verdejo, R.; Barroso-Bujans, F.; Rodriguez-Perez, M. A.; de Saja, J. A.; Lopez-Manchado, M. A. Functionalized graphene sheet filled silicone foam nanocomposites. *J. Mater. Chem.* **2008**, *18*, 2221.

(6) Lee, L. J.; Zeng, C. C.; Cao, X.; Han, X. M.; Shen, J.; Xu, G. J. Polymer nanocomposite foams. *Compos. Sci. Technol.* **2005**, *65*, 2344.

(7) Zeng, C.; Hossieny, N.; Zhang, C.; Wang, B. Synthesis and processing of PMMA carbon nanotube nanocomposite foams. *Polymer* **2010**, *51*, 655.

(8) Shen, J.; Han, X. M.; Lee, L. J. Nanoscaled reinforcement of polystyrene foams using carbon nanofibers. *J. Cell. Plast.* **2005**, *42*, 105.

(9) Ling, J. Q.; Zhai, W. T.; Feng, W. W.; Shen, B.; Zhang, J. F.; Zheng, W. G. Facile preparation of lightweight microcellular polyetherimide/graphene composite foams for electromagnetic interference shielding. *ACS Appl. Mater. Interfaces* **2013**, *5*, 2677.

(10) Chen, J. K.; Zhu, J.; Wang, J.; Yuan, M.; Chu, H. J. The properties of the Poisson's ratio of microcellular foams with low porosity: non-stationary, negative value, and singularity. *Mech. Time-Depend. Mater.* **2006**, *10*, 315.

(11) Siripurapu, S.; Gay, Y. J.; Royer, J. R.; DeSimone, J. M.; Spontak, R. J.; Khan, S. A. Generation of microcellular foams of PVDF and its blends using supercritical carbon dioxide in a continuous process. *Polymer* **2002**, *43*, 5511.

(12) Huang, H. X.; Wang, J. K.; Sun, X. H. Improving of cell structure of microcellular foams based on polypropylene/high-density polyethylene blends. *J. Cell. Plast.* **2008**, *44*, 69.
(13) Okamoto, M.; Nam, P. H.; Maiti, P.; Kotaka, T.; Nakayama, T.; Takada, M.; Ohshima, M.; Usuki, A.; Hasegawa, N.; Okamoto, H. Biaxial flow-induced alignment of silicate layers in polypropylene/clay nanocomposite foam. *Nano Lett.* **2001**, *1*, 503.
(14) Fu, J.; Naguib, H. E. Effect of nanoclay on the mechanical properties of PMMA/clay nanocomposite foams. *J. Cell. Plast.* **2006**, *42*, 325.
(15) Di, Y. W.; Iannace, S.; Di Maio, E.; Nicolais, L. Poly(lactic acid)/organoclay nanocomposites: thermal, rheological properties and foam processing. *J. Polym. Sci. Polym. Phys.* **2005**, *43*, 689.
(16) Zeng, C. C.; Han, X. M.; Lee, L. J.; Koelling, K. W.; Tomasko, D. L. Polymer-clay nanocomposite foams prepared using carbon dioxide. *Adv. Mater.* **2003**, *15*, 1743.
(17) Serhatkulu, G. K.; Dilek, C.; Gulari, E. Supercritical CO_2 intercalation of layered silicates. *J. Supercrit. Fluids* **2006**, *39*, 264.
(18) Lee, Y. H.; Wang, K. H.; Park, C. B.; Sain, M. Effects of clay dispersion on the foam morphology of LDPE/clay nanocomposites. *J. Appl. Polym. Sci.* **2007**, *103*, 2129.
(19) Zhang, H. B.; Zheng, W. G.; Yan, Q.; Jiang, Z. G.; Yu, Z. Z. The effect of surface chemistry of graphene on rheological and electrical properties of polymethylmethacrylate composites. *Carbon* **2012**, *50*, 5117.
(20) Thomassin, J. M.; Pagnoulle, C.; Bednarz, L.; Huynen, I.; Jerome, R.; Detrembleur, C. Foams of polycaprolactone/MWNT nanocomposites for efficient EMI reduction. *J. Mater. Chem.* **2008**, *18*, 792.
(21) Chen, L.; Ozisik, R.; Schadler, L. S. The influence of carbon nanotube aspect ratio on the foam morphology of MWNT/PMMA nanocomposite foams. *Polymer* **2010**, *51*, 2368.
(22) Yeh, J. M.; Chang, K. C.; Peng, C. W.; Lai, M. C.; Hung, C. B.; Hsu, S. C.; Hwang, S. S.; Lin, H. R. Effect of dispersion capability of organoclay on cellular structure and physical properties of PMMA/clay nanocomposite foams. *Mater. Chem. Phys.* **2009**, *115*, 744.
(23) Hwang, S. S.; Hsu, P. P.; Yeh, J. M.; Yang, J. P.; Chang, K. C.; Lai, Y. Z. Effect of clay and compatibilizer on the mechanical/thermal properties of microcellular injection molded low density polyethylene nanocomposites. *Int. J. Heat Mass Transfer* **2009**, *36*, 471.
(24) Veca, L. M.; Lu, F. S.; Meziani, M. J.; Cao, L.; Zhang, P. Y.; Qi, G.; Qu, L. W.; Shrestha, M.; Sun, Y. P. Polymer functionalization and solubilization of carbon nanosheets. *Chem. Commun.* **2009**, *18*, 2565.
(25) Potts, J. R.; Dreyer, D. R.; Bielawski, C. W.; Ruoff, R. S. Graphene-based polymer nanocomposites. *Polymer* **2011**, *52*, 5.
(26) Zhang, H. B.; Zheng, W. G.; Yan, Q.; Yang, Y.; Lu, Z. H.; Wang, J. W.; Ji, G. Y.; Yu, Z. Z. Electrically conductive polyethylene terephthalate/graphene nanocomposites prepared by melt compounding. *Polymer* **2010**, *51*, 1191.
(27) Yan, D. X.; Ren, P. G.; Pang, H.; Fu, Q.; Yang, M. B.; Li, Z. M. Efficient electromagnetic interference shielding of lightweight graphene/polystyrene composite. *J. Mater. Chem.* **2012**, *22*, 18772.
(28) Shen, B.; Zhai, W.; Tao, M.; Ling, J.; Zheng, W. G. Lightweight, multifunctional polyetherimide/graphene@Fe_3O_4 composite foams for shielding of electromagnetic pollution. *ACS Appl. Mater. Interfaces* **2013**, *5*, 11383.
(29) Li, C.; Yang, G.; Deng, H.; Wang, K.; Zhang, Q.; Chen, F.; Fu, Q. The preparation and properties of polystyrene/functionalized graphene nanocomposite foams using supercritical carbon dioxide. *Polym. Int.* **2013**, *62*, 1077.
(30) Chen, Z.; Xu, C.; Ma, C.; Ren, W.; Cheng, H. M. Lightweight and flexible graphene foam composites for high-performance electromagnetic interference shielding. *Adv. Mater.* **2013**, *25*, 1296.
(31) Chen, Z. P.; Ren, W. C.; Gao, L. B.; Liu, B. L.; Pei, S. F.; Cheng, H. M. Three-dimensional flexible and conductive interconnected graphene networks grown by chemical vapour deposition. *Nat. Mater.* **2011**, *10*, 424.
(32) Dong, X. C.; Wang, X. W.; Wang, L. H.; Song, H.; Zhang, H.; Huang, W.; Chen, P. 3D graphene foam as a monolithic and macroporous carbon electrode for electrochemical sensing. *ACS Appl. Mater. Interfaces* **2012**, *4*, 3129.
(33) Yang, J.; Wu, M.; Chen, F.; Fei, Z.; Zhong, M. Preparation, characterization, and supercritical carbon dioxide foaming of polystyrene/graphene oxide composites. *J. Supercrit. Fluids* **2011**, *56*, 201.
(34) Qi, X. Y.; Yan, D.; Jiang, Z. G.; Cao, Y. K.; Yu, Z. Z.; Yavari, F.; Koratkar, N. Enhanced electrical conductivity in polystyrene nanocomposites at ultra-low graphene content. *ACS Appl. Mater. Interfaces* **2011**, *3*, 3130.
(35) Ma, H. L.; Zhang, H. B.; Hu, Q. H.; Li, W. J.; Jiang, Z. G.; Yu, Z. Z.; Dasari, A. Functionalization and reduction of graphene oxide with p-phenylene diamine for electrically conductive and thermally stable polystyrene composites. *ACS Appl. Mater. Interfaces* **2012**, *4*, 1948.
(36) Bao, J. B.; Liu, T.; Zhao, L.; Hu, G. H. A two-step depressurization batch process for the formation of bi-modal cell structure polystyrene foams using $scCO_2$. *J. Supercrit. Fluids* **2011**, *55*, 1104.
(37) Yeh, S. K.; Huang, C. H.; Su, C. C.; Cheng, K. C.; Chuang, T. H.; Guo, W. J.; Wang, S. F. Effect of dispersion method and process variables on the properties of supercritical CO_2 foamed polystyrene/graphite nanocomposite foam. *Polym. Eng. Sci.* **2013**, *53*, 2061.
(38) Du, F. M.; Scogna, R. C.; Zhou, W.; Brand, S.; Fischer, J. E.; Winey, K. I. Nanotube networks in polymer nanocomposites: rheology and electrical conductivity. *Macromolecules* **2004**, *37*, 9048.
(39) Vermant, J.; Ceccia, S.; Dolgovskij, M. K.; Maffettone, P. L.; Macosko, C. W. Quantifying dispersion of layered nanocomposites via melt rheology. *J. Rheol.* **2007**, *51*, 429.
(40) Shen, J.; Zeng, C. C.; Lee, L. J. Synthesis of polystyrene-carbon nanofibers nanocomposite foams. *Polymer* **2005**, *46*, 5218.
(41) Zhu, B.; Zha, W. B.; Yang, J. T.; Zhang, C. L.; Lee, L. J. Layered-silicate based polystyrene nanocomposite microcellular foam using supercritical carbon dioxide as blowing agent. *Polymer* **2010**, *51*, 2177.